

# Phase behaviour and microstructure of partially-miscible, glass-forming, alcohol-water-maltotriose mixtures

Y. M. GUNNING, B. LALLOUE, T. R. NOEL, M. L. PARKER, R. PARKER, N. M. RIGBY

*Institute of Food Research, Food Materials Science Division, Norwich Research Park, Colney, Norwich NR4 7UA, UK*

*E-mail: Roger.parker@bbsrc.ac.uk*

The miscibility, occurrence of glass formation, and microstructure of maltotriose mixtures with water, methanol, ethanol, propan-1-ol and butan-1-ol at 20°C were studied. Maltotriose is fully miscible with water, but in binary mixtures, it is only partially miscible with short-chain alcohols. In methanol mixtures, the maltotriose-rich phase is a highly viscous liquid, but it is glassy in ethanol, propan-1-ol and butan-1-ol mixtures. In ternary alcohol-water-maltotriose mixtures, increasing water content increased miscibility, resulting in the progressive transformation of two phase liquid-glass mixtures into low viscosity single phase solutions. At water contents below about 4% w/w, the state diagram of ethanol-water-maltotriose mixtures includes a region of liquid-glass coexistence. Quenching single phase solutions into this region of the state diagram yielded aggregated dispersions of glassy particles, a process we term “glassy precipitation.”

© 2004 Kluwer Academic Publishers

## 1. Introduction

At low water contents, amorphous carbohydrates form glasses which occur both in natural systems, such as seeds and pollen [1, 2], and in man-made preservation and delivery systems, with applications to pharmaceuticals [3, 4], proteins [5] and flavours [6]. An appreciation of glass transition, e.g., Williams-Landel-Ferry (WLF) theory [7, 8], and water plasticization concepts [9,10] have underpinned the development and rational processing of these materials [9, 11].

State diagrams which summarise the temperatures and compositions at which liquid, crystalline and glassy states occur in binary carbohydrate-water mixtures have been characterised for many carbohydrates [12, 13]. In the absence of carbohydrate crystallisation and at sub-zero temperatures, water-rich mixtures contain co-existing phases of crystalline ice with either liquid or glassy freeze-concentrated carbohydrate solution. However, studies of the phase behaviour of carbohydrates in mixtures with poorer non-aqueous solvents are rare. Previous reports have described liquid-liquid separation (e.g., acetone-water-sucrose [14] and ethanol-water-maltose [6]) but the tendency of these carbohydrates to crystallise in low water content mixtures meant that glass formation was not studied. The physical situation involving the interaction of glass formation with liquid-liquid phase separation is relevant to diverse material processing technologies, for example, material-matrix interactions in encapsulation [6], separation processes in which glass formation is to be avoided [15] and

freeze-drying where a second water-immiscible volatile yields a glass with a desirable porous microstructure [16].

When a liquid carbohydrate-water mixture is vitrified, whether this is by quenching or drying, the very high viscosity, to a large extent, fixes its microstructure. Thus, common vitrification processes such as spray-drying and freeze-drying yield materials with structures characteristic of the processes which created them. Spray-dried materials consist of spherical particles, often with spherical voids created by vapour-inflated bubbles as the liquid boils prior to vitrification [17]. Freeze-dried water-rich solutions are microporous, the pores resulting from the sublimation of ice crystals during primary drying, the matrix having been vitrified by quenching and freeze-concentration in the initial cooling of the material [18]. With the appropriate temperature and composition data the paths which these processes follow can be concisely summarized as trajectories on the state diagram [19]. In the present study the state diagram indicates that it is possible to achieve vitrification by quenching a high temperature, single phase solution into the liquid-glass coexistence region of the phase diagram [20, 21], a process which we term “glassy precipitation”. This initial study demonstrates that this process yields a dispersion of glassy particles.

In this study, to facilitate the observation of the glassy state, the trisaccharide maltotriose which, to our knowledge, has never been known to crystallise [22] was chosen. The homologous series of short-chain alcohols

from methanol to *n*-butanol were used to examine the role of polarity on the solvent properties for the carbohydrate, both in binary mixtures and in ternary mixtures with water. The microstructures resulting from changing miscibility were studied by microscopy, the occurrence of glassy phases were monitored using differential scanning calorimetry and, when practical, the composition of coexisting phases were determined chromatographically. Finally, the microstructure of the precipitates which results when a mixture is quenched from a single phase region of the phase diagram into the liquid-liquid and liquid-glass coexistence regions were characterised.

## 2. Experimental

### 2.1. Materials

Maltotriose (>95.0% w/w) was obtained from Sigma Chemical Co. and methanol (>99.8% w/w), ethanol (>99.7% w/w), propan-1-ol (>99.5% w/w) and butan-1-ol (99.5% w/w) (all Analar grade) were obtained from BDH Chemicals Ltd. The maltotriose was ground then dried over P<sub>2</sub>O<sub>5</sub> in a vacuum oven at 60°C overnight. The alcohols were dried before use with molecular sieves (Sigma; pore size, 0.3 nm; 10% w/w). Formamide and Karl-Fischer reagent (pyridine free) were also obtained from BDH Chemical Ltd. Sodium tartrate dihydrate (Karl-Fischer standard) was obtained from Fluka Chemicals. All water for preparation of the mixtures and for preparing eluent for HPLC was taken from a water purifier (Elga, Elgastat Maxima; water resistivity, 18.2 MΩ cm). Sulphuric acid was from Reidel de Haen.

### 2.2. Mixture preparation

#### 2.2.1. Binary mixtures

2 g batches of 50% w/w maltotriose-water and the various maltotriose-alcohol mixtures were prepared by mixing maltotriose with the appropriate liquids in 10 mL screw-topped Pyrex tubes in a nitrogen-flushed glove-box. The mixtures were mixed using a vortex mixer, centrifuged for 25 min at 4500 rpm (3373 g) and held at 20°C for 15 days prior to analysis.

#### 2.2.2. Ternary mixtures

In general, 2 g batches of the ternary mixtures were prepared by mixing the required proportions of each component in 10 mL screw-topped Pyrex tubes. The mixtures were heated to 120°C in a pre-heated hot-block. For mixtures containing methanol (boiling point 64.6°C) and low amounts of water, the maltotriose and water were heated first to 120°C, cooled prior to the addition of the methanol and then the mixture reheated to 80°C. All the mixtures were mixed, centrifuged and stored at 20°C, as described for the binary mixtures.

#### 2.2.3. Preparation of precipitates

Ethanol-water-maltotriose solutions were prepared by first dissolving the maltotriose into the water, then

adding boiling ethanol, and finally heating the mixtures to 100°C in screw-topped Pyrex tubes until the maltotriose was completely dissolved (about 1 h). Ethanol-maltotriose mixtures were heated from cold and required frequent vortex mixing and prolonged heating (about 2 h) to achieve dissolution. Precipitates were prepared by quenching solutions from 100°C to room temperature by shaking the tubes whilst in a stream of cold tap water. The temperature dropped over 45 s giving a quench rate of about 1.8°C/s. The precipitates were stored overnight prior to microscopy and calorimetry.

### 2.3. Analysis of composition

#### 2.3.1. High performance liquid chromatography (HPLC)

Maltotriose and alcohol concentrations were measured using an HPLC (Gilson) equipped with a refractive index detector. Separation was achieved using an Aminex HPX-87H ion exclusion column (300 mm × 7.8 mm) (Bio-Rad) with a 12 mM sulphuric acid eluent at a flow-rate of 0.6 mL/min at 55°C. Samples were injected using a 10 μL loop. Duplicate measurements were made of each sample.

#### 2.3.2. Karl-Fischer titration

Water content was determined using a Baird and Tatlock AF5 Karl Fischer titrator. Calibration was by 25 μL injections of water and was checked using a 150 mg sample of sodium tartrate dihydrate (water content, 15.66% w/w). Samples were dissolved in a 2:1 v/v methanol-formamide solvent. Water contents were replicated to within 0.3% w/w.

### 2.4. Microscopy

Samples of turbid maltotriose-rich phase from the ternary mixtures were viewed using a Leitz Ortohix microscope with differential interference contrast optics. Droplet and particle sizes were determined by measuring large magnification images. The length scale was determined from images of a graticule photographed through the same optics as the sample. Sizes were averages over 20 measurements. Samples of the precipitates were viewed using a Olympus BX 60 microscope with bright field illumination.

### 2.5. Viscometry

A Bohlin Controlled Stress rheometer (model CS10) was used to measure viscosity in a parallel plate (20 mm diameter) geometry at shear stresses in the range 10–2000 Pa at 20°C. The surfaces of the sample exposed to the atmosphere were coated with a thin layer of silicone oil (Dow Corning 200/10 cS) to reduce evaporation.

### 2.6. Calorimetry

Glass transition temperatures ( $T_g$ ) of maltotriose-rich phases were determined using a Perkin-Elmer

DSC2 differential scanning calorimeter (DSC) fitted with a liquid-nitrogen, controlled-cooling accessory. The instrument was calibrated for temperature and heat flow using the melting of indium (Perkin-Elmer;  $T_m$ , 156.6°C;  $\Delta H$ , 28.45 Jg<sup>-1</sup>). Reusable high-pressure, stainless-steel capsules with copper sealing discs (Perkin-Elmer) were used for the precipitates as it was necessary to scan to temperatures in excess of the boiling points of the alcohols. The masses of the sample capsules were measured before and after scanning to verify that the capsules were sealed. The glass transition temperature was taken as the midpoint of the heat capacity increase which occurs at the glass transition on rescanning [23]. The scanning rate was 10 K min<sup>-1</sup>. Samples of precipitate were initially separated from the ethanol-rich phase by filtration in a glove box flushed with nitrogen and were then immediately sealed into DSC capsules to minimise both ethanol loss from the maltotriose-rich phase and water sorption from the atmosphere.

### 3. Results and discussion

#### 3.1. Binary mixtures of maltotriose

Fig. 1 shows the structure of binary mixtures (50% w/w) formed by maltotriose with water and short-chain alcohols (methanol to butan-1-ol) held at 20°C for 15 days. Table I shows literature values for the glass transition temperatures of pure water and alcohols. Their low values between -174°C and -137°C indicate that they are all potentially plasticizers of the maltotriose ( $T_g$ , 134°C). While the water mixture forms a single solution phase, the alcohol mixtures are all two phase with a transparent alcohol-rich upper phase and a maltotriose-rich lower phase. While the maltotriose-rich phase of the methanol mixture is a highly viscous liquid, the maltotriose-rich phase in the ethanol, propan-1-ol and butan-1-ol mixtures remains as discrete particles which can be dispersed throughout the liquid with agitation. The maltotriose content of the alcohol-rich phases (g maltotriose/100 g mixture) were determined as 16.3, 0.57, 0.10 and 0.03 for methanol, ethanol, propan-1-ol and butan-1-ol mixtures, respectively. The glass transition temperatures of the maltotriose-rich phases were determined as -19, 98, 99, 100°C, in the methanol, ethanol, propan-1-ol and butan-1-ol mixtures, respec-

TABLE I Glass transition temperatures of pure materials in this study

Material	$T_g$ (°C)
Water <sup>24</sup>	-137
Methanol <sup>24</sup>	-168
Ethanol <sup>24</sup>	-174
Propan-1-ol <sup>24</sup>	-169
Butan-1-ol <sup>24</sup>	-158
Maltotriose <sup>10</sup>	134

tively. The maltotriose-rich phase in the methanol mixture is above its glass transition at 20°C, whereas in the other alcohol mixtures this phase is glassy.

#### 3.2. Ternary alcohol-water-maltotriose mixtures

A continuous range of behaviour was observed when maltotriose was mixed in alcohol-water mixtures. Fig. 2 shows the effect of water content on the structure of a ternary mixture with equal amounts of ethanol and maltotriose. The behaviour of the sample with 15% w/w water was similar to that in pure methanol, with a transparent alcohol-rich upper phase and a turbid viscous maltotriose-rich lower phase. When the water content is increased to 20% w/w the lower maltotriose-rich phase becomes clear. During the preparation of this sample it was noted that, at 100°C this sample was single phase, thus the system has an upper critical solution temperature. Once the water content was increased to 25% w/w only a single liquid phase was present. For systems with two distinct liquid phases (e.g., 20% w/w water in Fig. 2) the composition of both phases were analysed, whereas in systems with turbid or glassy maltotriose-rich phases only the homogeneous alcohol-rich phase was analysed. Fig. 3a, b and c show the resulting ternary phase diagrams. The methanol mixtures only showed limited immiscibility at water contents below 10% w/w and were not analysed. Although water is fully miscible with maltotriose, methanol, ethanol and propan-1-ol, the ternary mixtures show only partial miscibility and for ethanol and propan-1-ol, water content has a strong influence on miscibility. The series shows the crossover in behaviour resulting from increasing hydrophobicity. For example, water partitions almost equally between

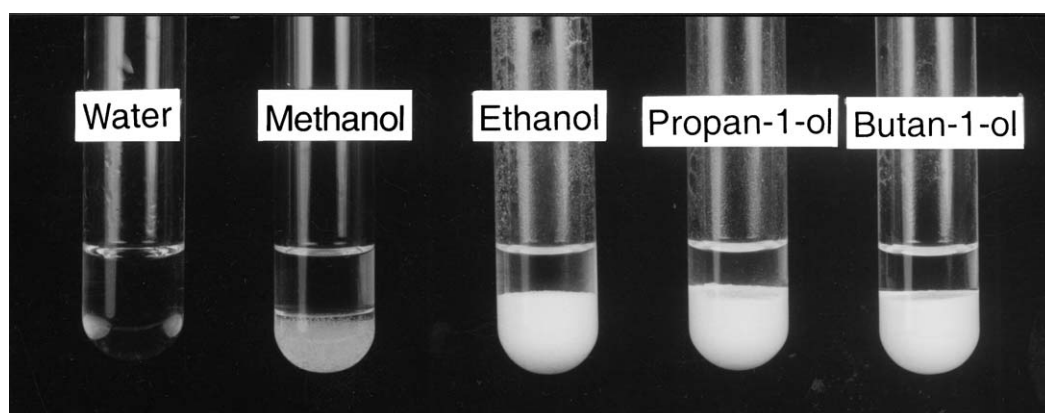


Figure 1 Binary 50% w/w mixtures of maltotriose with water and alcohols at 20°C.

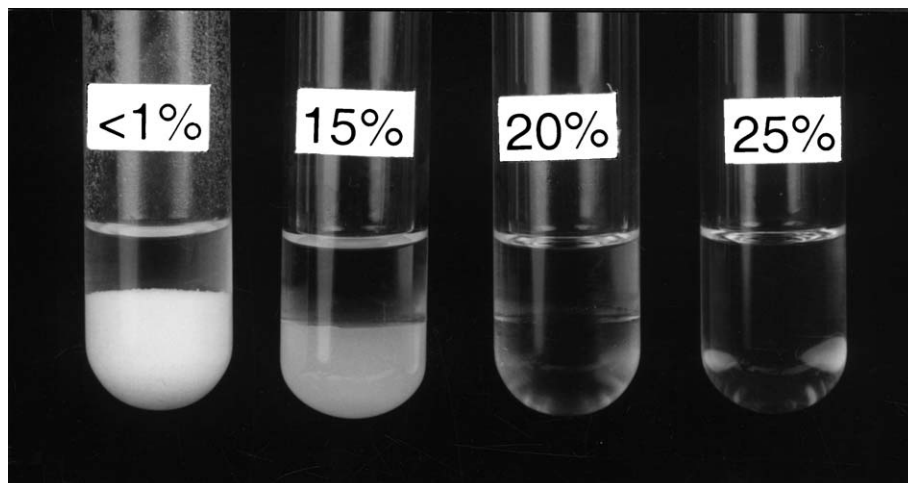


Figure 2 Ternary ethanol-water-maltotriose mixtures with varying amounts of water (% w/w) and equal ethanol and maltotriose contents at 20°C.

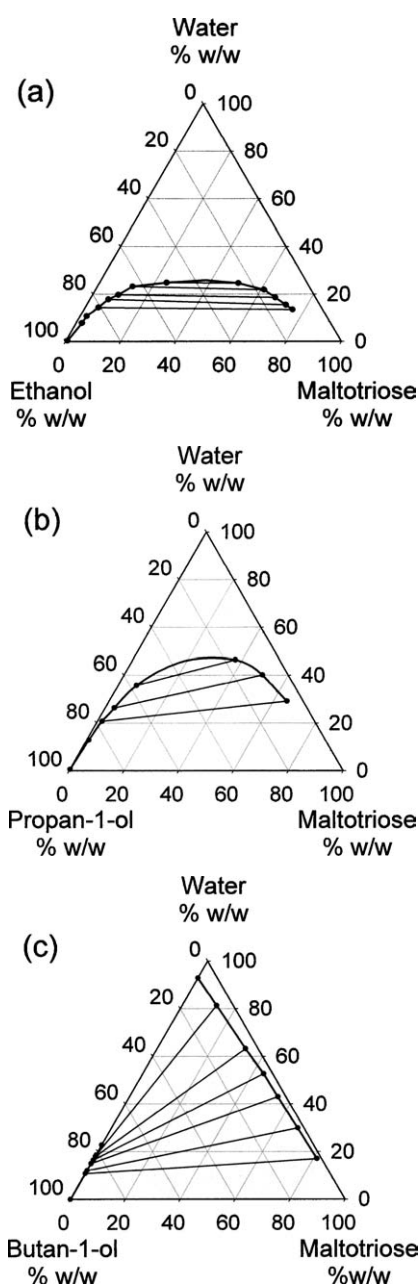


Figure 3 Ternary alcohol-water-maltotriose phase diagrams at 20°C for mixtures containing (a) ethanol, (b) propan-1-ol and (c) butan-1-ol, showing liquid-liquid coexistence curve with tie-lines joining coexisting phases.

the phases in the ethanol mixtures, whereas, for the butan-1-ol mixtures the water partitions predominantly into the maltotriose-rich phase.

The reasons for the occurrence of the turbidity in the maltotriose-rich phase of the ethanol-15% w/w water-maltotriose mixture (Fig. 2) were investigated using microscopy and viscometry. The phase is a coarse emulsion with droplet diameters in the range 5–15  $\mu\text{m}$ . The maltotriose-rich continuous phase had a Newtonian viscosity of about 20 Pa·s in the shear rate range 0.5–100  $\text{s}^{-1}$ . The slow creaming of these droplets is consistent with Stokes' law predictions i.e., the creaming velocity,  $v$ , is given by [25]

$$v = \frac{a^2 |\Delta\rho| g}{3\eta} \quad (1)$$

where,  $a$ , is the hydrodynamic radius,  $\Delta\rho$ , the density difference between the continuous and dispersed phases,  $g$ , the acceleration due to gravitation and  $\eta$  the viscosity of the continuous phase. 5  $\mu\text{m}$  diameter droplets of the ethanol-rich phase are predicted to cream at 0.5  $\mu\text{m}/\text{day}$ , i.e., they would take 200 days to traverse a 10 mm sample. Centrifugation was used to increase the creaming rate during the preparation of the mixtures. 25 min centrifugation at 3373  $g$ , is equivalent to 58 days of creaming at normal  $g$ -forces. While prolonged centrifugation allows higher viscosity samples to be separated, as the water content is lowered and the viscosity of the continuous phase increases, the creaming is ultimately so slow that the time for separation exceeds practical experimental timescales. To conclude, the turbidity is due to alcohol-rich droplets trapped in the viscous maltotriose-rich phase. This means that using the present techniques, the extent of the maltotriose-rich branch of the liquid-liquid coexistence curve is limited at lower water contents.

For the ethanol mixture the aim was to augment the phase diagram (Fig. 3a) to cover as large a composition range as practical. Dry maltotriose is glassy at 20°C and so the state diagram has a glassy region in the maltotriose corner, bounded by the curve describing compositions with a glass transition temperature of 20°C. Mixtures of maltotriose plasticised with between 5 and

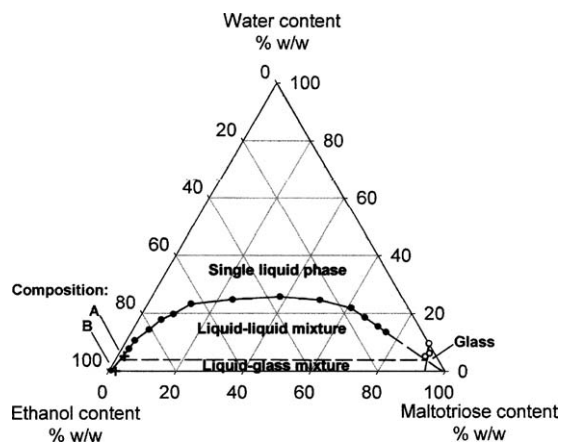


Figure 4 Ethanol-water-maltotriose state diagram at 20°C. Closed and open circles are compositions on the liquid-liquid coexistence and glass transition curves, respectively. Dashed lines are extrapolated, see text for details. Crosses are the compositions which were quenched to study their microstructure.

12% w/w water and 4:1 and 3:2 ethanol-water mixtures were scanned in the DSC and the composition at which the glass transition temperature occurred at 20°C was interpolated. The glass transition temperature of the plasticised maltotriose occurred at 20°C for a 9.7% w/w water mixture, 7.8% w/w for a 4:1 ethanol-water mixture and 8.6% for a 3:2 ethanol-water mixture. Scanning calorimetry of mixtures containing higher proportions of ethanol did not give clear glass transitions presumably due to poor mixing and phase separation effects. Combining the glass transition data together with the liquid-liquid coexistence data (Fig. 3a) allows a state diagram, Fig. 4, to be constructed. As explained above, over practical timescales, it is not possible to determine the maltotriose-rich branch of the liquid-liquid coexistence curve at compositions very close to the glass transition curve. For this reason this curve was linearly extrapolated using the available data. Similarly, it was not possible to determine the glass transition temperature at higher ethanol-water ratios and so the glass transition curve was linearly extrapolated from the maltotriose-water glass transition using the present data. These two lines intersect at the point 3.6% w/w ethanol, 3.9% w/w water, 92.5% w/w maltotriose. From this point the tie-line which divides liquid and glassy co-existing systems has been drawn. The data in Fig. 3a shows that the ratio of water contents in the maltotriose-rich and ethanol-rich phases remains constant at 0.94. Assuming that this ratio remains constant over the entire compositions range allows the water content of the ethanol-rich phase to be estimated as 4.1% w/w and the tie-line to be drawn.

### 3.3. Precipitation of highly viscous and glassy maltotriose-rich phases

The existence of an upper critical solution temperature for the 20% w/w water-ethanol-maltotriose mixture indicates that it is possible to quench from the single phase region of the phase diagram to a two phase region i.e., causing a liquid-liquid phase separation to occur. If the quench is performed for compositions within the liquid-

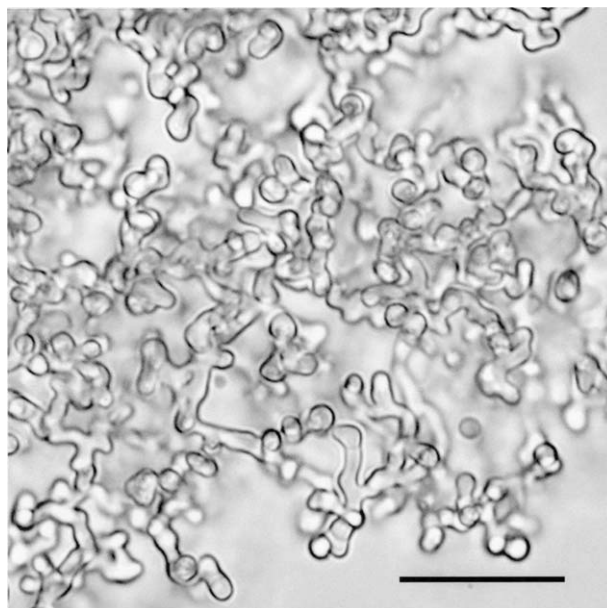


Figure 5 Structure of highly viscous maltotriose-rich precipitate in a quenched ethanol-water-maltotriose mixture of composition A: 92.8% w/w ethanol, 5.2% w/w water, 2.0% w/w maltotriose. Scale bar represents 20  $\mu\text{m}$ .

glass coexistence region the high viscosity of the glassy phase should arrest the phase separation process e.g., preventing coarsening by droplet-droplet coalescence. Precipitation experiments were performed by quenching solutions which were single phase at 100°C and had composition either side of the tie-line separating liquid-liquid separation and liquid-glass separation at 20°C i.e., mixtures with compositions: (A) 2.0% w/w maltotriose, 5.2% w/w water, and 92.8% w/w ethanol; and (B) 1.0% w/w maltotriose and 99.0% w/w ethanol. These compositions are indicated on Fig. 4. Single phase mixtures at 100°C only occurred at compositions close to the phase boundary in Fig. 4 i.e., the quenches are “off-critical”, away from the critical point and spinodal [20, 21, 26].

Fig. 5 shows the structure of an aggregate precipitated from the solution with composition A. The maltotriose-rich phase is above its glass transition temperature. The precipitating particles, typically about 3  $\mu\text{m}$  in diameter, have stuck together in an open aggregate structure which is undergoing a sintering-like, coalescence process. The process appears to be analogous to the stickiness of hygroscopic amorphous powders in which surface-tension driven flow is constrained by the viscosity of the liquid [27].

Fig. 6 shows a maltotriose-rich aggregate, about 60  $\mu\text{m}$  in diameter, which formed in the quenched solution with composition B. The glass transition temperature of the filtered aggregates was  $55 \pm 2^\circ\text{C}$  indicating that the material was in the glassy state at 20°C. In contrast to the behaviour observed in Fig. 5 it can be seen that the constituent spherical particles (2  $\mu\text{m}$  diameter) show limited coalescence. On vortex mixing the sedimented precipitate from composition B re-dispersed whereas that from composition A remained stuck to the wall of the test tube. While the phase structure in Fig. 6 shows that the maltotriose-rich precipitate

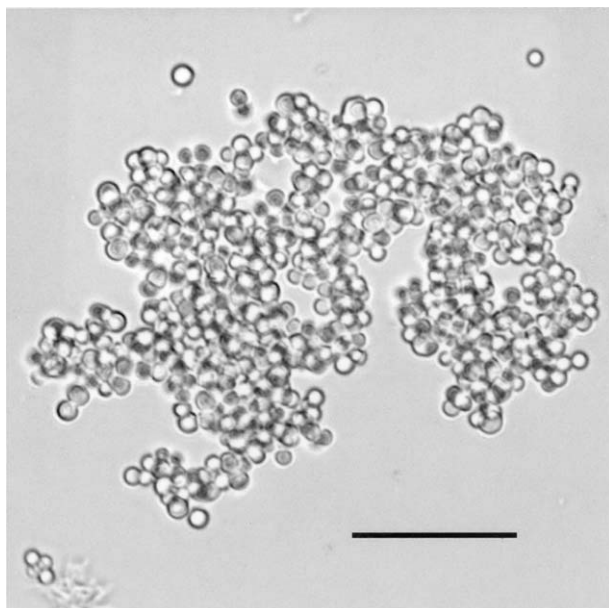


Figure 6 Structure of glassy maltotriose-rich aggregate in a quenched ethanol-maltotriose mixture of composition B: 99.0% w/w ethanol, 1.0% maltotriose. Scale bar represents 20  $\mu\text{m}$ .

has undergone considerable growth and aggregation during its formation, the calorimetric glass transition indicates that it has vitrified and its dispersibility we interpret as indicating that the glassy particles are no longer sticky or capable of surface-tension-driven flow. The non-equilibrium nature of the system is indicated by comparing the glass transition temperatures of the maltotriose-rich phase in the mixtures prepared by mixing dry maltotriose and ethanol (98°C, Section 3.1) and quenching a single phase maltotriose-ethanol solution (55°C, above). The lower glass transition temperature of the quenched sample reflects a higher ethanol content compared with the sample prepared by mixing i.e., the same steady state composition has not been achieved indicating a lack of equilibrium.

#### 4. Conclusions

The effect of varying the miscibility of plasticizing solvent and plasticizing solvent mixtures on the material behaviour of a glass-forming carbohydrate has been studied. These mixtures have states ranging from solutions and liquid-liquid mixtures to dispersions of glassy particles. The results demonstrate the intimate link between plasticizing solvent miscibility, glass formation and material behaviour. Quenching single phase solutions into the liquid-glass coexistence region resulted in aggregated dispersions of glassy particles. The aggregation and coarseness (2  $\mu\text{m}$  diameter) of the particles show that glass formation takes place late in the phase separation process. The ethanol-water-maltotriose state diagram, combining phase separation and glass formation, represents a new type of phase diagram for carbohydrates which has diverse applications in materi-

als processing e.g., flavour encapsulation [6], polymer fractionation [15] and freeze-drying [16].

#### Acknowledgements

YMG, TRN, MLP, RP and NMR acknowledge support of core strategic grants from the BBSRC and BL an EU grant under the Leonardo Da Vinci program.

#### References

1. J. H. CROWE, J. F. CARPENTER and L. M. CROWE, *Annu. Rev. Physiol.* **60** (1998) 73.
2. F. A. HOEKSTRA, E. A. GOLOVINA and J. BUITINK, *Trends Plant Sci.* **6** (2001) 431.
3. M. J. PIKAL, in "Amorphous Food and Pharmaceutical Systems," edited by H. Levine (RSC, Cambridge, 2002) p. 257.
4. D. LECHUGA-BALLESTEROS, in "Amorphous Food and Pharmaceutical Systems," edited by H. Levine (RSC, Cambridge, 2002) p. 275.
5. J. F. CARPENTER, S. J. PRESTRELSKI, T. J. ANCHORDOGUY and T. ARAKAWA, *ACS Symp. Ser.* **567** (1994) 134.
6. Y. M. GUNNING, R. PARKER, S. G. RING, N. M. RIGBY, B. WEGG and A. BLAKE, *J. Agric. Food. Chem.* **48** (2000) 395.
7. M. L. WILLIAMS, R. F. LANDEL and J. D. FERRY, *J. Amer. Chem. Soc.* **77** (1955) 3701.
8. J. D. FERRY, in "Viscoelastic Properties of Polymers" (Wiley, New York, 1980) p. 264.
9. H. LEVINE and L. SLADE, *Carbohydr. Polym.* **6** (1986) 213.
10. P. D. ORFORD, R. PARKER, S. G. RING and A. C. SMITH, *Int. J. Biol. Macromol.* **11** (1989) 91.
11. F. FRANKS, *Cryo-Lett.* **11** (1990) 93.
12. A. P. MACKENZIE, *Philos. Trans. Roy. Soc. B* **278** (1977) 167.
13. S. ABLETT, M. J. IZZARD and P. J. LILLFORD, *J. Chem. Soc., Fara. Trans.* **88** (1992) 789.
14. Z. BUBNIK and P. KADLEC, in "Sucrose Properties and Applications," edited by M. Mathlouthi and P. Reiser (Blackie, London, 1995) p. 101.
15. C. NEUHL and A. MERSMANN, *Chem. Eng. Sci.* **50** (1995) 951.
16. S. WITTAYA-AREEKUL and S. L. NAIL, *J. Pharm. Sci.* **87** (1988) 491.
17. M. ROSENBERG, Y. TALMON and I. J. KOPELMAN, *Food Microstr.* **7** (1988) 15.
18. C. VAN DEN BERG, F. FRANKS and P. ECHLIN, in "The Glassy State in Foods," edited by J. M. V. Blanshard and P. J. Lillford (Nottingham University Press, Nottingham, 1999) p. 249.
19. Y. ROOS and M. KAREL, *Food Techn.* **66** (1991) 68.
20. R. M. HIKMET, S. CALLISTER and A. KELLER, *Polymer* **29** (1988) 1378.
21. S. CALLISTER, A. KELLER and R. M. HIKMET, *Makromol. Chem., Macromol. Symp.* **39** (1990) 19.
22. W. PANGBORN, D. LANGS and S. PEREZ, *Int. J. Biol. Macromol.* **7** (1985) 363.
23. B. WUNDERLICH, "Thermal Analysis" (Academic Press, London, 1990) p. 101.
24. C. A. ANGELL, J. M. SARE and E. J. SARE, *J. Phys. Chem.* **82** (1978) 2622.
25. E. DICKINSON and G. STAINSBY, "Colloids in Food" (Applied Science Publishers, London, 1982) p. 146.
26. D. SAPPELT and J. JACKLE, *Physica A* **240** (1997) 453.
27. G. E. DOWNTON, J. L. FLORES-LUNA and J. C. KING, *Ind. Eng. Chem. Fund.* **21** (1983) 447.

Received 12 November 2003  
and accepted 2 August 2004